Naval Research Laboratory
Washington, DC 20375-5320

NRL/5650/MR—2023/1

Distortion Metrics for Multiple-Input, Single-Output Systems in Terms of Nonlinear Polynomial Coefficients

FRANK BUCHOLTZ

Jacobs Technology Incorporated
Herndon, VA

MATTHEW J. MONDICH
JOSEPH M. SINGLEY

Photonics Technology Branch
Optical Science Division

January 12, 2023

REPORT DOCUMENTATION PAGE

Form Approved
OMB No. 0704-0188

1. REPORT DATE *(DD-MM-YYYY)*	**2. REPORT TYPE**	**3. DATES COVERED** *(From - To)*
12-01-2023	NRL Memorandum Report	1 Oct 2021 – 31 July 2022

4. TITLE AND SUBTITLE

Distortion Metrics for Multiple-Input, Single-Output Systems in Terms of Nonlinear Polynomial Coefficients

5a. CONTRACT NUMBER

5b. GRANT NUMBER

5c. PROGRAM ELEMENT NUMBER

6. AUTHOR(S)

Frank Bucholtz*, Matthew J. Mondich, and Joseph M. Singley

5d. PROJECT NUMBER

5e. TASK NUMBER

5f. WORK UNIT NUMBER

6B50

7. PERFORMING ORGANIZATION NAME(S) AND ADDRESS(ES)

Naval Research Laboratory
4555 Overlook Avenue, SW
Washington, DC 20375-5320

8. PERFORMING ORGANIZATION REPORT NUMBER

NRL/5650/MR--2023/1

9. SPONSORING / MONITORING AGENCY NAME(S) AND ADDRESS(ES)

Office of Naval Research
One Liberty Center
875 North Randolph Street
Arlington, VA 22203-1995

10. SPONSOR / MONITOR'S ACRONYM(S)

ONR

11. SPONSOR / MONITOR'S REPORT NUMBER(S)

12. DISTRIBUTION / AVAILABILITY STATEMENT

DISTRIBUTION STATEMENT A: Approved for public release; distribution is unlimited.

13. SUPPLEMENTARY NOTES

*Jacobs Technology Incorporated, 2551 Dulles View Drive, Suite 700, Herndon, VA

14. ABSTRACT

The Navy has an interest in fiber-optic beamforming systems. Such systems comprise multiple RF inputs and a single RF output but where the signal processing is performed almost entirely in the optical domain and thus takes advantage of all the benefits of the single-mode fiber-optic technology including wide RF bandwidth and low RF loss. However, the theory of such multiple-input, single-output (MISO) photonic systems is not well developed.

As a prelude to an analysis of photonic beamforming systems, in this report we develop the mathematical foundation for the analysis of an RF-only MISO system. We assume every nonlinear element in the array can be modeled by a third-order polynomial and a standard noise model. Since the analysis is based on the the more-fundamental power-series expansion rather than the distortion metrics of each element, this approach will have broad applicability to both purely-RF and photonic beamforming systems.

15. SUBJECT TERMS

Multiple input Single output Intercept point
RF distortion Third-order distortion

16. SECURITY CLASSIFICATION OF:			**17. LIMITATION OF ABSTRACT**	**18. NUMBER OF PAGES**	**19a. NAME OF RESPONSIBLE PERSON**
a. REPORT	**b. ABSTRACT**	**c. THIS PAGE**			Frank Bucholtz
U	U	U	U	23	**19b. TELEPHONE NUMBER** *(include area code)* (410) 725-0642

Standard Form 298 (Rev. 8-98)
Prescribed by ANSI Std. Z39.18

This page intentionally left blank.

Contents

This page intentionally left blank.

1 EXECUTIVE SUMMARY

The Navy has an interest in fiber-optic beamforming systems. Such systems comprise multiple RF inputs and a single RF output but where the signal processing is performed almost entirely in the optical domain and thus takes advantage of all the benefits of the single-mode fiber-optic technology including wide RF bandwidth and low RF loss. However, the theory of such multiple-input, single-output (MISO) photonic systems is not well developed.

As a prelude to an analysis of photonic beamforming systems, in this report we develop the mathematical foundation for the analysis of an RF-only MISO system. We assume every nonlinear element in the array can be modeled by a third-order polynomial and a standard noise model. Since the analysis is based on the the more-fundamental power-series expansion rather than the distortion metrics of each element, this approach will have broad applicability to both purely-RF and photonic beamforming systems.

This page intentionally left blank.

2 Overview

Expressions for the overall gain and second- and third-order distortion metrics for a purely-RF system comprising a series arrangement of nonlinear elements are well known. However, certain system designs such as receive-mode beamformers and phased-arrays employ multiple, parallel signal paths, each containing multiple nonlinear elements (NLEs) that are summed together to produce a final output as shown in Fig.1. Such systems are referred to as multiple-input/single-output (MISO) systems.

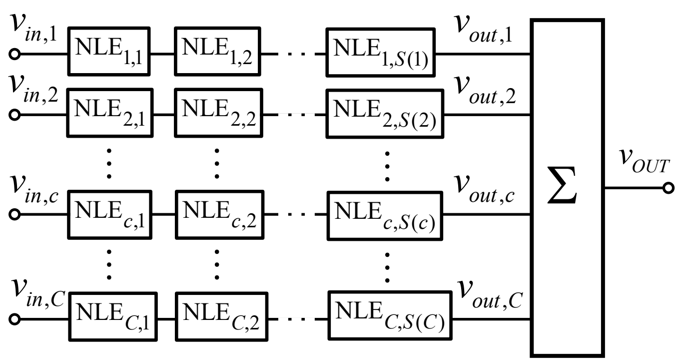

Figure 1: A generic RF multiple-input/single-output (MISO) system comprising C channels with input voltages $v_{in,c}$ $(1 \leq c \leq C)$ where each channel may comprise multiple nonlinear elements (NLEs) in series. $S(c)$ is the total number of series nonlinear elements in channel c and $NLE_{c,s}$ denotes the $s-$th element in series in the $c-$th channel. The C output voltages, one from each channel, $v_{out,c}$, are summed together to produce the final output v_{OUT}.

Various partial analyses of this type of system have appeared in the literature. Lee [1] obtained the noise figure and the antenna-gain-to-effective-temperature ratio (G/T) for a parallel, active-aperture array and mentions the possible use of mixed-technology RF/photonic systems for beamforming applications. Holzman *et al* [2] made a comparison of the gain, noise figure and output third-order intercept for active, passive and hybrid transmit/receive arrays and also calculated the general $m-$th order output intercept point for an active phased-array antenna [3]. Kraft [4] calculated the gain and G/T ratio for beamforming networks. Gatti *et al* [5] calculated the overall RF power gain, noise figure, and input third-order intercept point for an active antenna array. In all of these cases, the effective distortion metrics for the overall system were expressed in terms of distortion metrics of the individual elements or subsystems and none of the analyses included

Manuscript approved January 11, 2023.

second-order distortion or spurious-free dynamic range.

Simultaneous with the increased interest in active and passive multielement antenna systems over the past few decades came rapid progress in the development of fiber optic technology and thus the feasibility of mixed-technology systems, especially to utilize the large instantaneous bandwidth and low-loss, true-time delay capabilities of singlemode optical fiber. Several groups began analyzing such systems. Froberg *et al* [6] investigated the signal-to-noise ratio of a photonic beamformer. Recently, Mondich *et al* [7] investigated, both theoretically and experimentally, the gain and noise characteristics of a receive-mode photonic beamforming network. Many other works in the area of photonic beamformers and phased arrays can be found (see, for example, the references contained in [7].)

However, an issue arises in attempting to analyze mixed-technology systems with computational tools developed for purely-RF systems. For example, the third-order output intercept point $OIP3$ for an individual optical component in an RF photonic link cannot necessarily be defined in a way that is exactly analogous to the well-known and well-accepted definition of $OIP3$ for an RF component. It was this issue that motivated the current work.

In this paper we lay the foundation for analyses of the nonlinear behavior of multielement, mixed-technology, MISO systems. The basis of the approach is to represent the weak nonlinear behavior of any element, subsystem, or end-to-end system by a third-order polynomial

$$y = a_0 + a_1 x + a_2 x^2 + a_3 x^3 \tag{1}$$

relating output parameter y to input parameter x. This description is well known in RF design where the input and output parameters are both voltages. But the relationship in (1) is applicable generally to any input and output parameters provided, of course, that the coefficients a_i are defined properly. For example, (1) is a good model for the nonlinear response of an optical amplitude modulator where x is RF voltage and y is optical power.

In this work we calculate the overall, effective second-order output intercept point $OIP2$, third-order output intercept point $OIP3$, and third-order spurious-free dynamic range $SFDR3$ for the purely-RF system shown in Fig. 1 in terms of the nonlinear expansion coefficients $\{a_0, a_1, a_2, a_3\}$ of each individual element. Once expressions for the distortion metrics are known in terms of the $\{a_i\}$ coefficients, the expressions can be applied to any mixed-technology system, an extension that is beyond the scope of this paper. Here, we analyze only the purely-RF version of the system in Fig. 1 since all the fundamental results can be obtained under this simplifying assumption.

We adopt an obvious strategy. We first reduce the series cascade of NLEs in each path, or channel, to a single NLE characterized by a third-degree power series and we obtain explicit expressions for the nonlinear coefficients in this case. We then obtain the overall distortion metrics for a parallel array of single NLEs for an arbitrary number C of channels. Finally, we obtain the general expressions for the distortion metrics of the full array in (Fig. 1) in terms of the nonlinear polynomial coefficients of each of the individual elements.

3 Background

In this section we review i) the description of nonlinear behavior in terms of polynomial coefficients, and ii) the well-known expressions for $OIP2$ and $OIP3$ for both a single NLE and for a series cascade of NLEs, mainly to define terms and to establish nomenclature. In this section we also present new results in the form of expressions for the distortion metrics explicitly in terms of the polynomial coefficients a_1, a_2 and a_3.

3.1 Third-order Nonlinearity

Assume that the behavior of a NLE can be modelled by a third-degree polynomial (power series) relating output RF voltage v_{out} to input RF voltage v_{in},

$$v_{out} = a_1 v_{in} + a_2 v_{in}^2 + a_3 v_{in}^3, \tag{2}$$

where the nonlinear coefficients have dimensions $a_1 \propto$ (dimensionless), $a_2 \propto V^{-1}$, and $a_3 \propto V^{-2}$. In writing (2) we assume the nonlinearity is weak in the sense that a) terms in the response of order larger than three are insignificant, and b) to a good approximation the RF power gain at the fundamental frequency is a_1^2. We have also neglected the dc offset term a_0. Throughout the paper we will assume that the gain $|a_1| > 1$.

The distortion metrics are obtained under the assumption that each input voltage $v_{in,c}$ comprises two RF tones having equal amplitudes and slightly different and incommensurate frequencies,

$$v_{in} = v_0 \left(\sin \Omega_1 t + \sin \Omega_2 t\right). \tag{3}$$

With two incommensurate tones at the input, the output (2) comprises a discrete-frequency power spectrum with tones at a number of frequencies. The list in Table I provides the voltage amplitude for the output frequencies that will be relevant in the subsequent analysis [8, 9].

Table 1: List of relevant output frequencies and voltage amplitudes

Frequency	**Amplitude (V)**
$(\Omega_{1,2})$	$a_1 v_0 + (9/4) a_3 v_0^3$
$(\Omega_2 \pm \Omega_1)$	$a_2 v_0^2$
$(2\Omega_{2,1} \pm \Omega_{1,2})$	$(3/4) a_3 v_0^3$

The assumptions in (2) and (3) combined with the results in Table 1 lead to the well-known results [8, 9] for average RF power gain (G), second-order output intercept point ($OIP2$), third-order output intercept point ($OIP3$), and normalized third-order spurious-free dynamic range ($SFDR3$),

$$G = a_1^2, \tag{4a}$$

$$OIP2 = \frac{1}{2R}\frac{a_1^4}{a_2^2}, \tag{4b}$$

$$OIP3 = \frac{2}{3R}\frac{a_1^3}{a_3}, \tag{4c}$$

$$SFDR3 = \left(\frac{OIP3}{\mathcal{N}_0}\right)^{2/3}, \tag{4d}$$

where R is the output load resistance and $\mathcal{N}_0$ is the output noise power spectral density (PSD) (W/Hz). For the RF gain we have assumed that input and output load resistances are equal.

If, on the other hand, G, $OIP2$, and $OIP3$ are known *a priori*, then the corresponding nonlinear coefficients can be obtained as

$$a_1 = G^{1/2}, \tag{5a}$$

$$a_2 = \left(\frac{1}{2R}\right)^{1/2} \frac{G}{OIP2^{1/2}}, \tag{5b}$$

$$a_3 = \left(\frac{2}{3R}\right) \frac{G^{3/2}}{OIP3}. \tag{5c}$$

3.2 General Results for Series Cascade of Elements

For a series cascade of S nonlinear devices, the worst-case $n-$th order nonlinear behavior can be approximated by the well-known series cascade formula [9]

$$OIPn_{ser}^r = OIPn_S^r + \left(G_S \cdot OIPn_{(S-1)}\right)^r + \ldots + \left(G_S G_{S-1} \cdots G_2 \cdot OIPn_1\right)^r, \tag{6}$$

where $r = (1-n)/2$, G_s is the RF power gain of the $s-$th element, and $n = 2, 3$ for second- and third-order OIP, respectively. That is, the serial array of NLEs shown in Fig. 2 can be replaced by a single NLE with effective $OIP2$ and $OIP3$ given by (6) with the appropriate choice of n. But since the $OIPn$ of each element can be written in terms of the a_i $(i = 1, 2, 3)$ for each element, the effective $OIPn$ for the serial cascade can

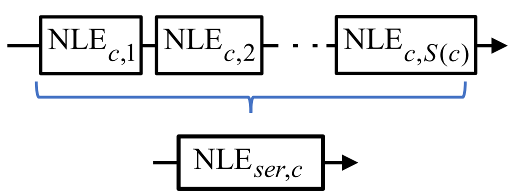

Figure 2: The well-known replacement of a series cascade of nonlinear elements by a single nonlinear element in which $OIP2$ and $OIP3$ are given in terms of the gains and intercept points of the individual NLEs by (6).

also be written in terms of the a_i's. After some algebra, it is easy to show that for $S = 3$ NLEs in series,

$$G_{ser}(3) = a_{1ser}^2(3), \tag{7a}$$

$$OIP2_{ser}(3) = \frac{1}{2R}\frac{a_{1ser}^4(3)}{a_{2ser}^2(3)}, \tag{7b}$$

$$OIP3_{ser}(3) = \frac{2}{3R}\frac{a_{1ser}^3(3)}{a_{3ser}(3)}, \tag{7c}$$

$$SFDR3_{ser}(3) = \left(\frac{OIP3_{ser}(3)}{\mathcal{N}_{0,ser}(3)}\right)^{2/3} \tag{7d}$$

where $G_{ser}(S)$, $OIP2_{ser}(S)$, $OIP3_{ser}(S)$ and $SFDR3_{ser}(S)$ denote the effective gain, $OIP2$, $OIP3$, and $SFDR3$, respectively, for a serial array of S

elements, and where

$$a_{1ser} = a_{1,3}a_{1,2}a_{1,1}, \tag{8a}$$

$$\begin{aligned} a_{2ser} = &\left(a_{1,2}^2 a_{1,1}^2\right) a_{2,3} \\ &+ \left(a_{1,3} a_{1,1}^2\right) a_{2,2} \\ &\quad + \left(a_{1,3} a_{1,2}\right) a_{2,1}, \end{aligned} \tag{8b}$$

$$\begin{aligned} a_{3ser} = &\left(a_{1,2}^3 a_{1,1}^3\right) a_{3,3} \\ &+ \left(a_{1,3} a_{1,1}^3\right) a_{3,2} \\ &\quad + \left(a_{1,3} a_{1,2}\right) a_{3,1}. \end{aligned} \tag{8c}$$

Here $a_{k,s}$ indicates the a_k coefficient of the s-th element in series. The coefficient $a_{3,2}$, for example, is a_3 in the power series expansion for the second ($s = 2$) element in series.

In general, for an arbitrary number S of elements in series, $OIP2$ and $OIP3$ can always be written in the form of (7b) and (7c) where a_{1ser} is the product of the individual $a_{1,s}$ coefficients and a_{2ser} and a_{3ser} are linear combinations of the $a_{2,s}$ and $a_{3,s}$ coefficients, respectively. We find

$$G_{ser}(S) = a_{1ser}^2(S), \tag{9a}$$

$$OIP2_{ser}(S) = \frac{1}{2R}\frac{a_{1ser}^4(S)}{a_{2ser}^2(S)}, \tag{9b}$$

$$OIP3_{ser}(S) = \frac{2}{3R}\frac{a_{1ser}^3(S)}{a_{3ser}(S)}, \tag{9c}$$

$$SFDR3_{ser}(S) = \left(\frac{OIP3_{ser}(S)}{\mathcal{N}_{0,ser}(S)}\right)^{2/3}, \tag{9d}$$

where

$$a_{1ser}(S) = \prod_{s=1}^{S} a_{1,s}, \tag{10a}$$

$$a_{2ser}(S) = \sum_{s=1}^{S} A_{2,s}(S)a_{2,s}, \tag{10b}$$

$$a_{3ser}(S) = \sum_{s=1}^{S} A_{3,s}(S)a_{3,s}. \tag{10c}$$

The weighting coefficients $A_{2,s}(S)$ and $A_{3,s}(S)$ are functions entirely of the linear gain coefficients $a_{1,s}$,

$$A_{2,s}(S) = \left(\prod_{p=1}^{s-1} a_{1,p}^2\right)\left(\prod_{q=s+1}^{S} a_{1,q}\right), \tag{11a}$$

$$A_{3,s}(S) = \left(\prod_{p=1}^{s-1} a_{1,p}^3\right)\left(\prod_{q=s+1}^{S} a_{1,q}\right). \tag{11b}$$

To obtain these results, we calculated directly the quantities a_{1ser}, a_{2ser} and a_{3ser} for $S = 2, 3, 4$. From these results the pattern for arbitrary S is quite clear and the general results can be written succinctly as in (11).

To evaluate $SDFR3$ in the general case it is necessary to choose a model to describe the noise. As a specific example suppose we make the standard assumption that, for a single RF device, the output noise PSD is characterized by a noise factor $F \geq 1$ such that

$$\mathcal{N}_0 = k_B T_0 a_1^2 F \tag{12}$$

where k_B is the Boltzman constant and $T_0 = 290K$ is the standard temperature. Then (4d) becomes

$$SFDR3 = \left[\frac{2}{3R}\frac{1}{k_B T_0 F}\frac{a_1}{a_3}\right]^{2/3}. \tag{13}$$

The noise PSD for a serial array of S elements is then obtained using (12) but with the replacements $a_1 \to a_{1,ser}(S)$ and $F \to F_{ser}(S)$ where $F_{ser}(S)$ is given by the well-known cascade formula

$$\begin{aligned} F_{ser}(S) =& F_1 + \frac{F_2 - 1}{a_{1,1}^2} + \frac{F_3 - 1}{(a_{1,1}a_{1,2})^2} + \cdots \\ & \cdots + \frac{F_S - 1}{(a_{1,1}a_{1,2}\cdots a_{1,S-1})^2} \\ =& \begin{cases} F_1 & S = 1 \\ F_1 + \sum_{s=2}^{S} \frac{F_s - 1}{\prod_{q=1}^{s-1} a_{1,q}^2} & S \geq 2. \end{cases} \end{aligned} \tag{14}$$

Then

$$\mathcal{N}_{0,ser}(S) = k_B T_0 G_{ser}(S) F_{ser}(S). \tag{15}$$

3.3 Limiting Cases: All Element Identical and $S >> 1$

For the purpose of comparison with the parallel case, it will be convenient to obtain expressions for the series metrics in the limiting case where all devices in the array are identical and characterized by the same set of parameters $\{a_1, a_2, a_3, F\}$. We further examine the behavior of the metrics in the limit of a large number of identical elements in each channel ($S >> 1$).

3.3.1 Serial Gain

The overall gain is simply the product of the individual, identical RF power gains,

$$G_{ser}^{ident}(S) = a_1^{2S}. \tag{16}$$

for all values $S \geq 1$.

3.3.2 Serial $OIP2$

The serial $OIP2$, after some algebra, is given in this case by

$$OIP2_{ser}^{ident}(S) = OIP2 \cdot \left[a_1^{(S-1)} \frac{(a_1 - 1)}{(a_1^S - 1)} \right]^2. \tag{17}$$

It is degraded from the $OIP2$ of each element by a factor that depends on the voltage gain a_1 and the total number of elements in series, S. In the limit of large S,

$$OIP2_{ser}^{ident}(S) \xrightarrow[S>>1]{\cdot} OIP2 \left(1 - \frac{1}{a_1} \right)^2. \tag{18}$$

That is, in the limit of a large number S of elements in series the cascade $OIP2$ approaches the individual $OIP2$ but reduced by the fixed factor $(1 - 1/a_1)^2$.

3.3.3 Serial $OIP3$

Again after some algebra, we find that the series-cascaded $OIP3$ for identical elements,

$$OIP3_{ser}^{ident}(S) = OIP3 \left(a_1^{2(S-1)} \frac{a_1^2 - 1}{a_1^{2S} - 1} \right), \tag{19}$$

is degraded from the $OIP3$ of each element by a factor that depends on the power gain a_1^2 and on the total number S of elements in series. Note that the number S of elements enters the degradation factor exponentially, just as it did for $OIP2$. In the limit of large S,

$$OIP3_{ser}^{ident}(S) \xrightarrow[S>>1]{\cdot} OIP3\left(1-\frac{1}{a_1^2}\right). \tag{20}$$

3.3.4 Serial $SFDR3$

To calculate $SFDR3$ for identical elements we first obtain the effective serial noise factor. Now

$$\prod_{q=1}^{s-1} a_1^2 = (a_1^2)^{s-1} \tag{21}$$

and so

$$\begin{aligned} F_{ser}^{ident}(S) &= F + (F-1)\sum_{s=2}^{S}\frac{1}{(a_1^2)^{s-1}} \\ &= F\left\{1+\left(\frac{F-1}{F}\right)\left[\frac{1-a_1^{-2(S-1)}}{a_1^2-1}\right]\right\}. \end{aligned} \tag{22}$$

In the limit of large S,

$$F_{ser}^{ident}(S) \xrightarrow[S>>1]{\cdot} F\left\{1+\left(\frac{F-1}{F}\right)\left[\frac{1}{a_1^2-1}\right]\right\}. \tag{23}$$

Use this result together with (16) and (15) to obtain the output noise PSD,

$$\mathcal{N}_{0,ser}^{ident}(S) = k_B T_0 G_{ser}^{ident}(S) F_{ser}^{ident}(S) \tag{24}$$

and, finally,

$$SFDR3_{ser}^{ident}(S) = \left[\frac{OIP3_{ser}^{ident}(S)}{\mathcal{N}_{0,ser}^{ident}(S)}\right]^{2/3} \tag{25}$$

where $G_{ser}^{ident}(S)$, $OIP3_{ser}^{ident}(S)$ and $\mathcal{N}_{0,ser}^{ident}(S)$ are given by (16), (19) and (24), respectively. Then

$$SFDR3_{ser}^{ident}(S) = \frac{SFDR3}{\mathcal{Q}_{ser}^{ident}(a_1, F, S)} \tag{26}$$

where $SFDR3$ for any individual device is given by (4d) and where the factor

$$\mathcal{Q}_{ser}^{ident}(a_1, F, S) = \left[\left(\frac{a_1^{2S}-1}{a_1^2-1}\right)\cdots\right.$$
$$\left.\cdots\left\{1+\left(\frac{F-1}{F}\right)\left[\frac{1-a_1^{-2(S-1)}}{a_1^2-1}\right]\right\}\right]^{2/3}. \tag{27}$$

For fixed gain a_1^2 and in the limit of large S we find a result that is expected but not particularly interesting, namely,

$$SFDR3_{ser}^{ident}(S) \xrightarrow[S>>1]{\cdot} 0, \tag{28}$$

even if $F = 1$.

From (17) and (19) note that the "correction" factors for $OIP2$ and $OIP3$ in the large S regime depend only on the voltage gain a_1 and the number of elements S and are independent of the nonlinear coefficients a_2 and a_3. The correction for $SFDR3$ depends on a_1, S and F but, again, is independent of the nonlinear coefficients. This occurs because of the significant implicit assumption that is made universally in this type of RF calculation, namely, that the distortion signals arise organically in each NLE due only to the strength of the fundamental at the element's input. Distortion signals due to higher-order mixing products are neglected.

In Fig. 3 we plot the ratios a) $OIP2_{ser}^{ident}(S)/OIP2$, b) $OIP3_{ser}^{ident}(S)/OIP3$, c) F/F_0, d) $\mathcal{N}_{0,ser}/\mathcal{N}_0$, and e) $SFDR3_{ser}^{ident}(S)/SFDR3$ assuming $F_0 = 1.35\,(NF_0 = 1.3dB)$, plotting the results for two gain values $a_1^2 = 10$ and 1000. Here,

$$\mathcal{N}_0 = k_B T_0 a_1^2 F_0. \tag{29}$$

Although the serial-cascade formulas for $m-$th order output-intercept point $OIPm$ and noise factor F are ubiquitous in textbooks and papers, the serial-cascade $SFDR$ in (26) and (27) is rarely found, perhaps because it requires the additional concept of noise model. Hence we remark that, whereas $OIPm$ and F degrade gracefully to a limiting value as S increases (Fig. 3 (a), (b), (c)), the output noise PSD increases as a_1^S (Fig. 3 (d)) and, as a result, the $SFDR3$ degrades rapidly at a rate $\sim (a_1^{-S})^{2/3}$ as more and more identical elements are added in series, Fig. 3 (e).

Finally, we note that in subsequent calculations, when a cascade serial quantity in (10) refers to a particular channel in the full array, say the

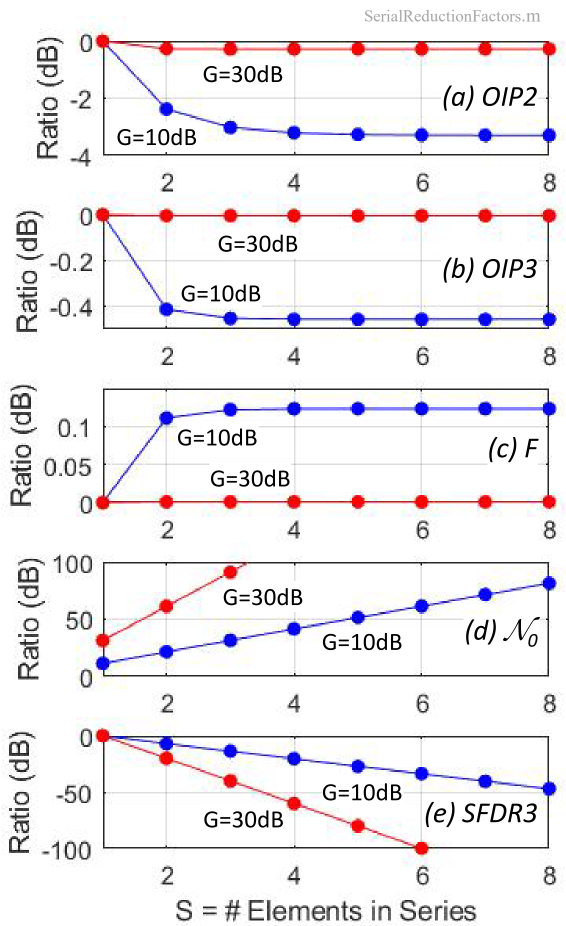

Figure 3: For a serial array of identical elements, these are plots of the ratios (dB) (a) $OIP2_{ser}^{ident}/OIP2$ from Eq.(17), (b) $OIP3_{ser}^{ident}/OIP3$ from Eq. (19), (c) the noise factor F_{ser}^{ident}/F_0, (d) $\mathcal{N}_{0,ser}/\mathcal{N}_0$ from (24) and (29), and (e) $SFDR3_{ser}^{ident}/SFDR3$ from Eq. (27) as a function of the number S of array elements assuming $F = 1.35$. Each graph comprises two plots corresponding to RF power gains $G = 10dB$ and $G = 30dB$. Here $OIP2$, $OIP3$ and $SFDR3$ refer to the values for any one element in the array. Note the vastly different vertical scales among the plots.

$c-$th channel, then we will add an index c to the subscript. For example, $a_{2ser,c}$ denotes the equivalent series-cascade a_2 coefficient for channel c with corresponding index added in the subscript to the quantities $a_{1,s} \to a_{1,s,c}$, and $A_{2,s} \to A_{2,s,c}$, etc.

4 Distortion Metrics for a Parallel Coherent Array

4.1 Multiple, Independent Parallel Inputs

We now consider the system shown in Fig. 4(a) in which C coherent input signals each pass through a given channel containing nonlinear elements in series and are then summed together. Assume the summing device is a Wilkinson-type device so the output voltage is given by

$$v_{OUT} = \sum_{c=1}^{C} \frac{v_{out,n}}{\sqrt{C}}. \tag{30}$$

Recall that the approach here is to a) reduce the system in Fig. 1 to an equivalent system in which each path contains only one equivalent element as shown in Fig. 4(a), and then to b) further reduce the parallel array to a

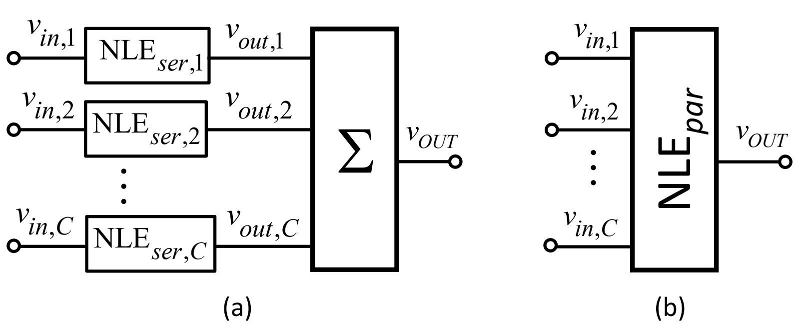

Figure 4: (a) Reduction of the MISO system in Fig. 1 to a system in which each input path contains only a single, effective series nonlinear element ($NLE_{ser,c}$); (b) Further reduction of the system in (a) to a single, equivalent parallel nonlinear element NLE_{par} where NLE_{par} now includes the intrinsic loss of the Wilkinson summer (30). In (a), note that $NLE_{ser,c}$ refers to the functionally-equivalent nonlinear element with coefficients obtained from a series-cascade analysis of the elements comprising that channel.

functionally-equivalent single nonlinear element having multiple inputs and a single output as shown in Fig. 4(b). For the system in Fig. 4(a) we have, from (2) and (30),

$$v_{OUT} = \frac{1}{\sqrt{C}} \left(\sum_{c=1}^{C} a_{1ser,c} v_{in,c} + \sum_{c=1}^{C} a_{2ser,c} v_{in,c}^2 \right.$$
$$\left. + \sum_{c=1}^{C} a_{3ser,c} v_{in,c}^3 \right) \tag{31}$$

where we have made the important assumption that the summing device operates linearly for all values $v_{in,c}$ of interest.

We next calculate $OIP2$, $OIP3$, and $SFDR3$ for the parallel array, again assuming the standard model for output noise.

4.2 Parallel OIP2

$OIP2$ is defined as the output power at which the linear extrapolation of the small-signal output power at either fundamental frequency intercepts the quadratic extrapolation of either second-order distortion term at $(\Omega_1 \pm \Omega_2)$. Hence, using the results in Table 1, at $OIP2$,

$$\frac{1}{2R} \left(\frac{v_0}{\sqrt{C}} \sum_{c=1}^{C} a_{1ser,c} \right)^2 = \frac{1}{2R} \left(\frac{v_0^2}{\sqrt{C}} \sum_{c=1}^{C} a_{2ser,c} \right)^2 \tag{32}$$

from which

$$OIP2_{par}(C) = \frac{1}{C} \frac{1}{2R} \frac{a_{1par}^4(C)}{a_{2par}^2(C)} \tag{33}$$

where

$$a_{1par}(C) = \sum_{c=1}^{C} a_{1ser,c}, \tag{34a}$$

$$a_{2par}(C) = \sum_{c=1}^{C} a_{2ser,c} \tag{34b}$$

and where, recall, $a_{1ser,c}$ and $a_{2ser,c}$ are given by (10a) and (10b), respectively.

If the C channels are all identical so that $a_{1ser,c} = a_{1ser}$ and $a_{2ser,c} = a_{2ser}$, for all c, then

$$a_{1par}^{ident}(C) = C \cdot a_{1ser}, \tag{35a}$$

$$a_{2par}^{ident}(C) = C \cdot a_{2ser}. \tag{35b}$$

Hence,

$$\begin{aligned} OIP2_{par}^{ident}(C) =& C \cdot \left(\frac{1}{2R} \frac{a_{1ser}^4}{a_{2ser}^2} \right) \\ =& C \cdot OIP2_{ser}. \end{aligned} \tag{36}$$

Thus the effective $OIP2$ of a parallel array of C identical channels, where $OIP2_{ser}$ denotes the serial $OIP2$ of each channel scales linearly with the number of channels, C. This can be compared to the very different behavior of a serial array where the number of elements S appeared in the exponent of various terms in the expression for $OIP2_{ser}$ as in (17).

It should be noted that the assumption of identical channels here does not imply the much stronger assumption that all NLE's in the array are identical, only that the series-cascade equivalent of the corresponding non-linear coefficients are equal. Of course, if all the elements in the array *are* identical then each channel is identical.

4.3 Parallel OIP3

$OIP3$ is defined as the output power at which the linear extrapolation of the small-signal output power at either fundamental frequency intercepts the cubic extrapolation of either third-order intermodulation product. Hence, using the results in Table 1, at $OIP3$ it is true that,

$$\frac{1}{2R} \left(\frac{v_0}{\sqrt{C}} \sum_{c=1}^{C} a_{1ser,c} \right)^2 = \frac{1}{2R} \left(\frac{3v_0^3}{4\sqrt{C}} \sum_{c=1}^{C} a_{3ser,c} \right)^2 \tag{37}$$

from which

$$OIP3_{par}(C) = \frac{1}{C} \frac{2}{3R} \frac{a_{1par}^3(C)}{a_{3par}(C)}, \tag{38}$$

where

$$a_{3par}(C) = \sum_{c=1}^{C} a_{3ser,c}. \tag{39}$$

In the case where all the channels are identical,

$$a_{3par}^{ident}(C) = C \cdot a_{3ser}, \tag{40}$$

and so

$$OIP3_{par}^{ident}(C) = C \cdot OIP3_{ser}. \tag{41}$$

Again, just as for $OIP2_{par}^{ident}$, the effective $OIP3$ for a parallel array of C identical channels scales linearly with C. The same result was obtained by Gatti [5].

4.4 Parallel Spurious-free Dynamic Range

For the parallel array, the third-order spurious-free dynamic range, designated here by $SFDR3_{par}(Hz^{2/3})$ is defined by [8]

$$SFDR3_{par}(C) = \left(\frac{OIP3_{par}(C)}{\mathcal{N}_{0,par}(C)} \right)^{2/3}. \tag{42}$$

where $\mathcal{N}_{0,par}(C)$ is the total output noise power spectral density due to all channels and all sources. An expression for $\mathcal{N}_{0,par}(C)$ can be written only after a specific noise model is chosen.

For purely-RF systems, in a previous report [10] we analyzed a parallel system of the type shown in Fig. 4(a) in which the single device in each input path was characterized by RF power gain $a^2_{1ser,c}$ and noise factor $F_{ser,c}$. We found that the total output noise power spectral density is given by

$$\mathcal{N}_{0,par}(C) = k_B T_0 \left[1 + \sum_{c=1}^{C} \left(\frac{F_{ser,c} a^2_{1ser,c} - 1}{C} \right) \right]. \tag{43}$$

Then, using (38) and (43), Eq. (42) provides the equivalent $SFDR3$ of the entire array in Fig. 1 when reduced to a single nonlinear element (Fig. 4). Hence, the parallel $SFDR3_{par}$ depends not only on the $a_{1,k}$ and $a_{3,k}$ polynomial coefficients of every element in the array but also, of course, on the noise characteristics of each element. (Note: In the report [10] the equation (43) included terms corresponding to linear loss $\mathcal{L}_{ser,c}$ in each channel. Those terms have been neglected in the calculation here for clarity.)

If all elements are identical, then (43) becomes

$$\mathcal{N}^{ident}_{0,par}(C) = k_B T_0 F_{ser} a^2_{1ser} = \mathcal{N}_{o,ser}(C) \tag{44}$$

which indicates that the noise factor of the parallel array is equal to the noise factor F_{ser} of any single channel in the array. This is consistent with the result obtained by Gatti [5].

Finally, the spurious-free dynamic range becomes

$$\begin{aligned} SFDR3^{ident}_{par} &= \left(\frac{OIP3^{ident}_{par}(C)}{\mathcal{N}^{ident}_{o,ser}(C)} \right)^{2/3} \\ &= C^{2/3} \cdot SFDR3_{ser}. \end{aligned} \tag{45}$$

Hence, the $SFDR3$ for a parallel array of identical channels scales as $C^{2/3}$ times the $SFDR3_{ser}$ of any one channel. Figure 5 shows the ratios for the parallel case corresponding to serial case shown in Fig. 3 where, now, the distortion metrics improve with additional, identical channels rather than degrading with additional identical elements. The three plots, corresponding to equations (36), (41), and (45), respectively, are thus nearly trivial but, when compared with Fig. 3, they illustrate the dramatically different behavior of a parallel array to a serial array. Importantly, we see that there is no penalty whatsoever for a parallel architecture *provided* the summing junction operates as a Wilkinson device.

5 Summary

We have obtained the second- and third-order distortion metrics for a multiple-input/single-output RF array in terms of the third-order polynomial coefficients and the output noise spectral density. In the equations below, $\{a_{1,c,s}, a_{2,c,s}, a_{3,c,s}\}$ denotes the set of nonlinear polynomial coefficients corresponding to the NLE in the $s-$th serial position in channel c. In summary,

$$OIP2_{par}(C) = \frac{1}{C}\frac{1}{2R}\frac{a_{1par}^4(C)}{a_{2par}^2(C)}, \tag{46a}$$

$$OIP3_{par}(C) = \frac{1}{C}\frac{2}{3R}\frac{a_{1par}^3(C)}{a_{3par}(C)}, \tag{46b}$$

$$SFDR3_{par}(C) = \left(\frac{OIP3_{par}(C)}{\mathcal{N}_{o,par}(C)}\right)^{2/3}, \tag{46c}$$

where

$$a_{1par}(C) = \sum_{c=1}^{C} a_{1ser,c}, \tag{47a}$$

$$a_{2par}(C) = \sum_{c=1}^{C} a_{2ser,c}, \tag{47b}$$

$$a_{3par}(C) = \sum_{c=1}^{C} a_{3ser,c}, \tag{47c}$$

$$\mathcal{N}_{o,par}(C) = \text{model dependent.} \tag{47d}$$

Here,

$$a_{1ser,c}(S(c)) = \prod_{s=1}^{S(c)} a_{1,s,c}, \tag{48a}$$

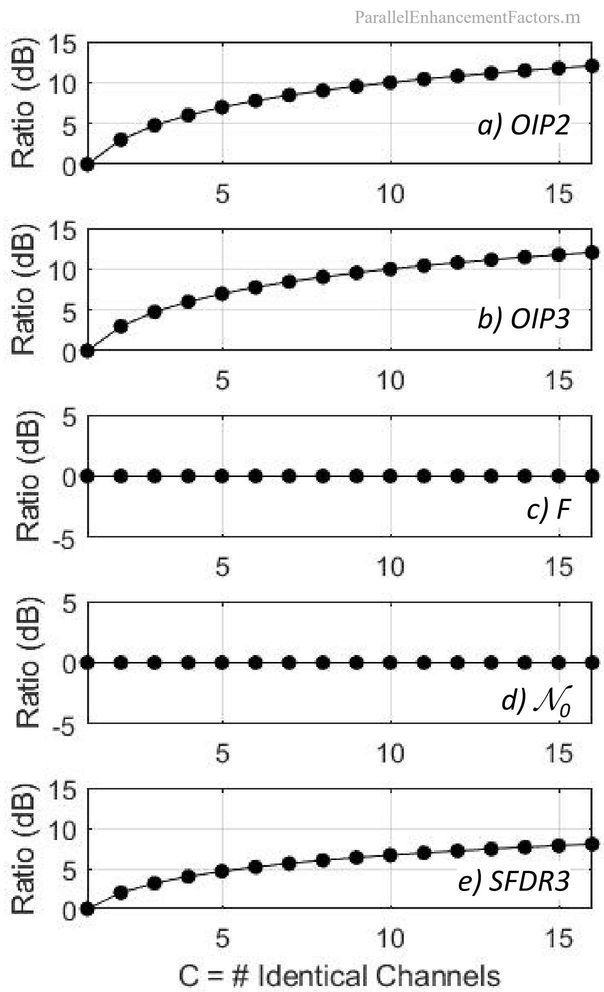

Figure 5: The same five ratios of Fig. 3 but here for a parallel array of C identical channels. The variation as a function of C is independent of the characteristics of any channel but does assume the summing junction is a Wilkinson device.

$$a_{2ser,c}(S(c)) = \sum_{s=1}^{S(c)} A_{2,s,c}(S(c))a_{2,s,c}, \tag{48b}$$

$$a_{3ser,c}(S(c)) = \sum_{s=1}^{S(c)} A_{3,s,c}(S(c))a_{3,s}, \tag{48c}$$

where, recall, $S(c)$ denotes the number of elements in series in channel c and where

$$A_{2,s,c}(S(c)) = \left(\prod_{p=1}^{s-1} a_{1,p,c}^2\right)\left(\prod_{q=s+1}^{S(c)} a_{1,q,c}\right), \tag{49a}$$

$$A_{3,s,c}(S(c)) = \left(\prod_{p=1}^{s-1} a_{1,p,c}^3\right)\left(\prod_{q=s+1}^{S(c)} a_{1,q,c}\right). \tag{49b}$$

As mentioned earlier, in general the form of the output noise $\mathcal{N}_0$ depends on the specific noise model chosen. In the case of a purely-RF system and assuming the standard noise model then equations $\mathcal{N}_{0,par}(C)$ is given by (43).

Although derived within the context of a purely-RF system, these equations are completely general and applicable to any mixed-technology multiple-input/single-output system because they are based on the completely generic cubic polynomial model (1) for nonlinearity. That is, to the extent that (1) is a good nonlinear model for each of the individual elements in the system, (46)-(49) together represent a good model for the nonlinear behavior of the entire MISO system.

Acknowledgment

The authors wish to acknowledge the Office of Naval Research for partial funding of this work under an NRL 6.2 Base Program.

References

[1] J.J. Lee. “G/T and noise figure of active array antenna”. *IEEE Trans. Ant. Prop.* **41**(2) (1993), pp. 241–244.

[2] E.L. Holzman and A.K. Agrawal. “A comparison of active phased array, corporate beamforming architectures”. *IEEE Proc. Intl. Symp. on Phased Array Systems and Technology* (1996), pp. 429–434.

[3] E.L. Holzman. “Intercept points of active phased array antennas”. *IEEE MTT-S Intnl. Microwave Symp. Digest* 2 (1996), pp. 999–1002.

[4] U.R. Kraft. “Gain and *G/T* of multielement receive antennas with active beamforming networks”. *IEEE Trans. Ant. Prop.* **48**(11) (2000), pp. 1818–1829.

[5] R.V Gatti, M. Diogini, and R. Sorrentino. “Computation of gain, noise figure, and third-order intercept of active array antennas”. *IEEE Trans. Ant. Prop.* **52**(11) (2004), pp. 3139–3142.

[6] N.M. Froberg, E.I Ackerman, and C.H. Cox, III. “Analysis of signal to noise ratio in photonic beamformers”. *IEEE 2006 Aerospace Conference* (12 pages) (2006).

[7] M.J. Mondich, J.D. McKinney, J.M. Singley, I.M. Maize, and K.J. Williams. “Group delay-based wideband photonic receive-mode radio-frequency beamforming”. *J. Lightwave Technol.* **38**(21) (2020), pp. 5893–5907.

[8] D.M. Pozar. Microwave Engineering, 4th ed. 2012.

[9] S.A. Maas. Nonlinear Microwave and RF Circuits, 2nd ed.

[10] F. Bucholtz, M.J. Mondich, J.M. Singley, J.D. McKinney, and K.J. Williams. “The Noise Figure for Multiple-Input RF Systems”. *U.S. Naval Research Laboratory Memorandum Report* 5651-20-10-10,103, Aug 28, 2020 (2020).